ISSN 1330-3651 (Print), ISSN 1848-6339 (Online)
UDC/UDK 621.833.058:[519.6:004.421]

NUMERICAL AND EXPERIMENTAL ANALYSIS OF THE CYCLOID DISC STRESS STATE

Mirko Blagojevic, Nenad Marjanovic, Zorica Djordjevic, Blaza Stojanovic, Vesna Marjanovic, Rodoljub Vujanac, Aleksandar Disic

Original scientific paper
The paper deals with the stress state analysis of the cycloid disc by using numerical and experimental methods for the most critical case of the meshing - single meshing. Cycloid disc is the vital element of the cycloidal speed reducer - mechanical power transmission of the new generation with growing use in industrial practice. 3D computer model of one specific one-stage cycloidal speed reducer was made. After that, the whole series of different numerical models of the cycloid disc were defined in FEMAP and NASTRAN, in order to determine the most realistic stress state by using FEM. In order to verify the results obtained by numerical methods, experimental analysis was realised using the strain gauges method. Physical model of the cycloid disc was made and also models of other elements of the cycloidal speed reducer which are in direct contact with it, in order to obtain the most realistic conditions for the experimental analysis. Obtained experimental results showed good agreement with numerical results. Even for the most unfavourable case of the theoretical meshing (single meshing), which is almost non-existent in practice, stress values are in allowed limits and provide reliable functioning of the reducer in the foreseen work life period.

***Keywords**: cycloid disc, cycloidal speed reducer, experimental analysis, numerical analysis*

Numerička i eksperimentalna analiza stanja naprezanja ciklozupčanika

Izvorni znanstveni članak
U ovom radu izvršena je analiza stanja naprezanja ciklozupčanika numeričkim i eksperimentalnim metodama za najkritičniji slučaj sprezanja – slučaj jednostrukog zahvata. Ciklozupčanik predstavlja vitalni element cikloreduktora – mehaničkog prijenosnika snage i gibanja novije generacije sa sve većom primjenom u industrijskoj praksi. Izrađen je 3D kompjuterski model jednog konkretnog jednostupanjskog cikloreduktora. Zatim je definiran čitav niz različitih numeričkih modela ciklozupčanika u programskim paketima FEMAP i NASTRAN radi određivanja što realnijeg stanja naprezanja uporabom metode konačnih elemenata (MKE). U cilju verifikacije dobivenih rezultata numeričkim putem, izvršena je eksperimentalna analiza korištenjem metode mjernih traka. Napravljen je fizički model ciklozupčanika kao i ostalih elemenata cikloreduktora koji su s njim u direktnom kontaktu kako bi se dobili što realniji uvjeti u postupku eksperimentalne analize. Dobiveni eksperimentalni rezultati pokazuju dobru sukladnost s numeričkim rezultatima. Čak i za najnepovoljniji teorijski slučaj sprezanja (jednostruki zahvat), koji se kod cikloreduktora u praksi gotovo i ne javlja, vrijednosti naprezanja su u dopuštenim granicama i osiguravaju pouzdan rad prijenosnika tijekom predviđenog radnog vijeka.

***Ključne riječi**: cikloreduktor, ciklozupčanik, eksperimentalna analiza, numerička analiza*

1 Introduction

Cycloidal speed reducers belong to the mechanical power transmission of the new generation. Their most important work characteristics are:

- Extremely wide range of possible gear ratios,
- Quiet and reliable work,
- Low level of noise and vibration,
- Exceptionally compact design,
- High efficiency rate,
- Almost complete absence of the lateral clearances.

Due to the fact that over 60 % of the cycloidal speed reducer elements which transmit the load, are in constant contact, this type of the power transmission can withhold impact overloads of short duration, even as high as 500 %. The listed cycloidal speed reducer characteristics enabled their wide application, such as in: robotics industry, transport devices, process equipment, food processing machines, mixers, satellites, etc.

Kudrijavcev described in details cycloidal speed reducers [1]. In his PhD, Lehmann [2] defined the method for calculation of forces that act upon the cycloid disc for the theoretical case, when there are no lateral clearances. Malhotra deduced analytical expressions for calculation of the power losses and efficiency rate [3]. Litvin and Feng paid special attention to the generation of the teeth profile of the cycloid disc (equidistant of shortened epicycloid) [4]. Yang and Blanche [5] analyzed the effects of machining tolerances on backlash and torque ripples.

In modern practice, it is usual to combine numerical and theoretical methods to obtain high quality and reliable results [6, 7, 8]. Numerical analysis results of the stress - strain state of the vital elements of the cycloidal speed reducer are presented in [9, 10, 11, 12, 13]. Meng, Wu and Ling included friction in the load analysis at cycloidal speed reducers and realised the whole series of experimental investigations [14]. Gorla and other defined expressions for the calculation of load and efficiency rate, for the newly developed type of the cycloidal speed reducer [15]. The paper also presented the whole list of experimental investigation results. Sensinger [16] developed a new method for cycloid drive profile, efficiency and stress optimization. Analysis of forces and moments in gerotor pumps is presented in [17].

In so far published papers, stress - strain state analysis of cycloidal speed reducer elements is done in the case when a half of cycloid disc teeth are in contact with rollers of the stationary central gear and transmit the load. However, this represents a theoretical case of meshing with no clearances between the mentioned elements. The existence of clearances is necessary to provide adequate lubricating conditions, as well as for the proper assembly and disassembly of the reducer.

This paper presents stress state analysis of the cycloid disc for the particular single-stage cycloidal speed reducer, in case of the single meshing (the most critical case), by using finite elements method (FEM). Also,

experimental analysis of the same meshing case is done, using the strain gauges method.

2 Cycloid disc loads

Intersection of the single-stage cycloidal speed reducer is shown in Fig. 1. Cycloid disc is the most important element of the reducer (due to its complex geometry, but also due to its extremely complex stress-strain state).

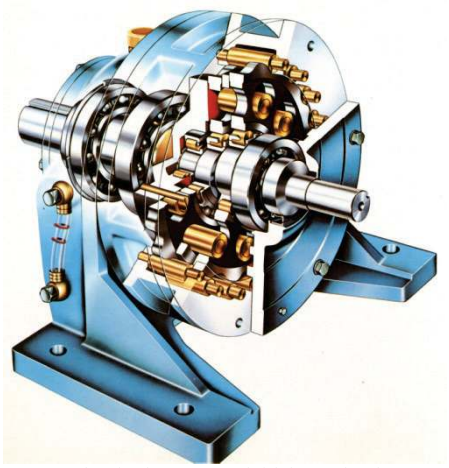

Figure 1 The single-stage cycloidal speed reducer

In order to analyse the stress state of the cycloid disc, it is necessary to know the loads that act upon it and they are shown in Fig. 2:
T_1 – drive torque,
T_2 – torque on the stationary central gear,
T_3 – output torque,
F_E – bearing reaction,
F_{Ni} – normal force in the current contact point between the cycloid disc tooth and the roller of stationary central gear,
F_{Kj} – normal force in the current contact point between the output roller and the hole in the cycloid disc.

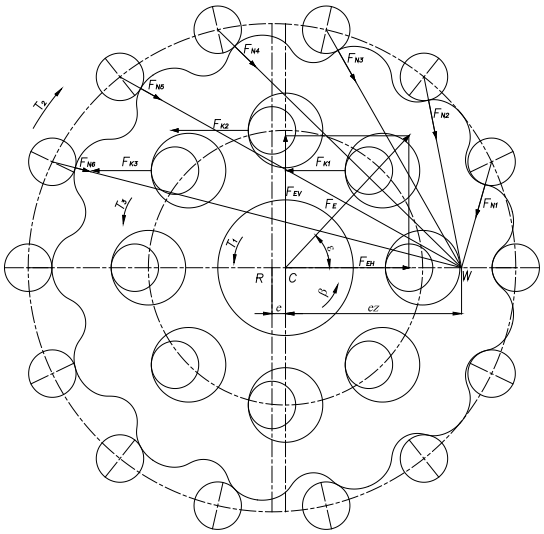

Figure 2 Cycloid disc loads

Torques and forces equilibrium equations of the cycloid disc are defined by expressions (1) and (2):

$$T_1 - T_2 + T_3 = 0 \tag{1}$$

$$\vec{F}_E + \sum_i \vec{F}_{Ni} + \sum_j \vec{F}_{Kj} = 0. \tag{2}$$

Loads calculation procedure for the cycloid disc is described in details in [1, 2, 3, 9, 11].

In theoretical case, when the reducer has no clearances, all cycloid disc teeth are in contact with appropriate rollers and half of them participate in the load transmission process. However, in reality, this is not the case. The existence of the clearances in the cycloidal speed reducer is necessary due to many reasons, some of which are:

- To compensate errors made during the manufacturing process of the reducer,
- To provide better lubricating conditions,
- To be able to realise the assembly and disassembly of the reducer.

Size of the clearances directly influences the number of cycloid disc teeth and appropriate rollers of the stationary central gear, which are in direct contact and transmit the loads. With clearance increase, the number of loaded teeth (rollers) decreases.

In this paper, stress state analysis of the cycloid disc is done, by using numerical and experimental methods for the most critical case of the meshing (single meshing). 3D model of one particular single-stage cycloidal speed reducer is made (Fig. 3) with the following characteristics:

- Input power P_{in} = 5,5 kW
- Input number of revolutions n_{in} = 1500 1/min
- Gear ratio u = 11
- Number of cycloid disc teeth z = 11
- Eccentricity e = 4 mm.

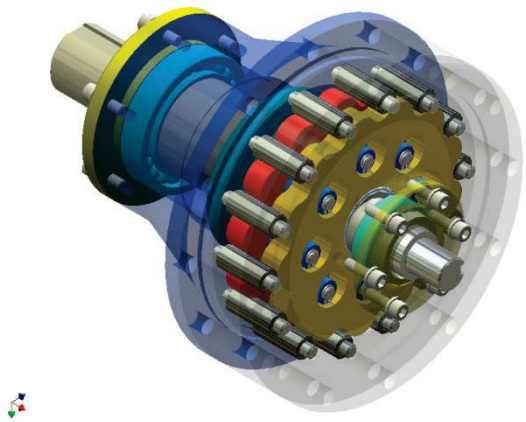

Figure 3 3D model of the investigated single-stage cycloidal speed reducer

3 Numerical analysis

Stress state analysis of the cycloid disc is realized using Finite Elements Method - FEM. For this purpose, the whole range of numerical models has been made. Cycloid disc is considered to be a deformable elastic body. It is considered that at one instant two output rollers

are in contact with a cycloid disc for all numerical models. Supports have been set up at these points. Bearing reaction F_E is decomposed into nine components and supports have been set up also at points of these components. External load is normal force F_N. Value of this force is calculated according to the procedures described elsewhere [1, 2, 3, 9, 11] and is $F_N = 4630$ N.

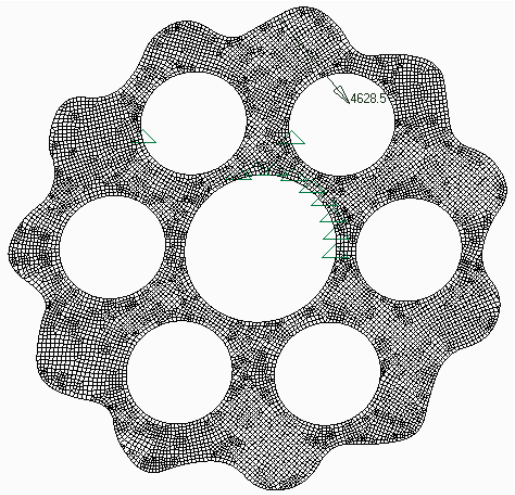

Figure 4 Numerical model of the cycloid disc with proposed limitations and loads

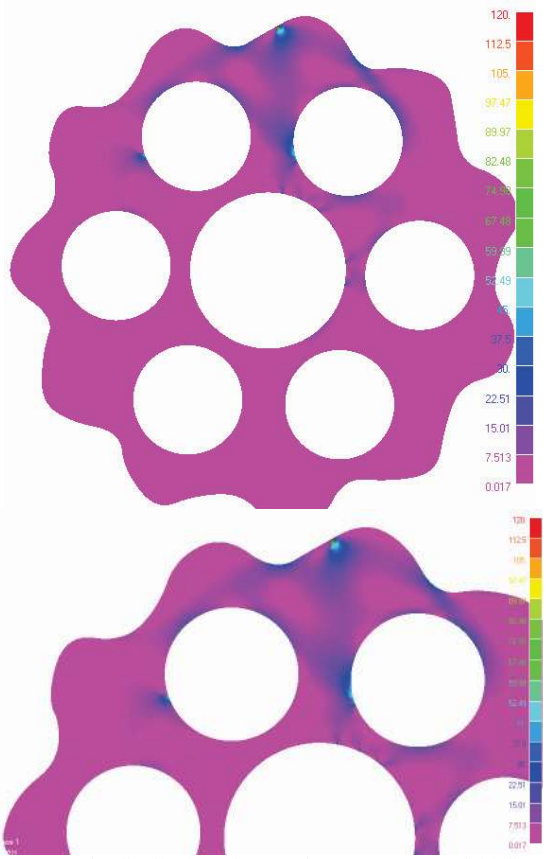

Figure 5 The distribution of Von-Mises stresses at cycloid disc

The problem is considered to be planar (Fig. 4). Quadrilateral two-dimensional isoparametric finite elements have been used. Cycloid disc model consisted of 9227 finite elements and 9753 nodes. Steel 30CrMoV9 (WNr 1.7707) was selected as a cycloid disc material, with the following characteristics: Yield stress (R_{eh} = 700 MPa), Tensile strength (R_m = 1100 MPa), Modulus of elasticity (E = 2,1×10^5 MPa), Poisson ratio (μ = 0,3). FEMAP and NASTRAN software was used for analysis. The distribution of Von-Mises stresses is shown in Fig. 5.

It can be clearly seen from Fig. 5, that the maximum value of the Von-Mises stress (σ_{max} = 120 MPa) occurred at the contact point of the cycloid disc tooth and the roller of the stationary central gear, as it was expected. Stress values in other zones of the cycloid disc are significantly lower than the maximum value.

The tooth root stress values are rather low, due to concave - convex shape of the teeth with cycloid profile, and can be neglected accordingly. This is one of the best advantages of the cycloid disc.

4 Experimental analysis

In order to verify stress state results obtained by using Finite Elements Method (FEM), experimental analysis was done. Cycloid disc was made with parameters given in Tab. 1. Also, appropriate cycloidal speed reducers elements were made, with which the cycloid disc is in immediate or relative contact.

Table 1 Main characteristics of the cycloid disc

Number of teeth	11
Material: steel	20MoCr4
Width, mm	13,3
Dedendum diameter, mm	116
Addendum diameter, mm	132
Eccentricity, mm	4

In order to completely simulate the situation of the meshing between the cycloid disc and rollers of the stationary central gear and with output rollers, the support was made that connected all the mentioned elements into one assembly (Figs. 6 and 7). The case of single meshing was analysed (only one tooth of the cycloid disc and appropriate roller of the stationary central gear are in contact), while the load is transmitted from the cycloid disc to the output shaft over the two output rollers. Input shaft with eccentricity is turned for the angle of 20°. External load acts upon the contact of the cycloid disc tooth and central gear rollers.

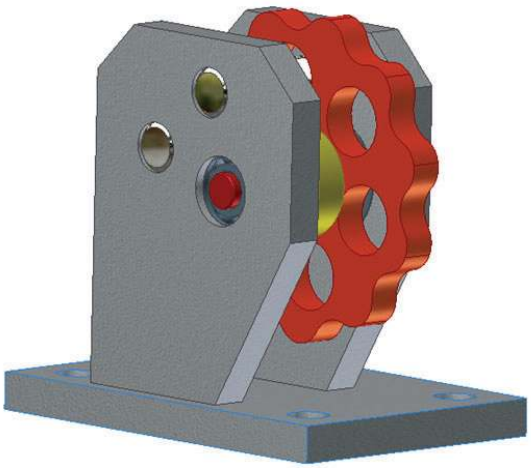

Figure 6 Computer model of the tool for investigation of the stress state of the cycloid disc

Maximum stresses at cycloid disc occur in the zone of its contact with the rollers of the central gear, output rollers and rollers of the needle bearings, at the position where the cycloid disc leans on the eccentricity. Due to the extremely favourable shape of the cycloid disc tooth, bending stresses at the tooth root are present in a very small extent and can be neglected. Contact stresses are also not very large, because the meshing is mostly concave - convex for the cycloidal gearing. Investigations showed that precisely in the contact zones where normal force has the maximum value, equivalent curve radius also has maximum value, what is exceptionally favourable from the aspect of the cycloid disc capacity. Also, at cycloidal speed reducers, larger number of teeth is always in simultaneous contact, what represents yet another significant advantage.

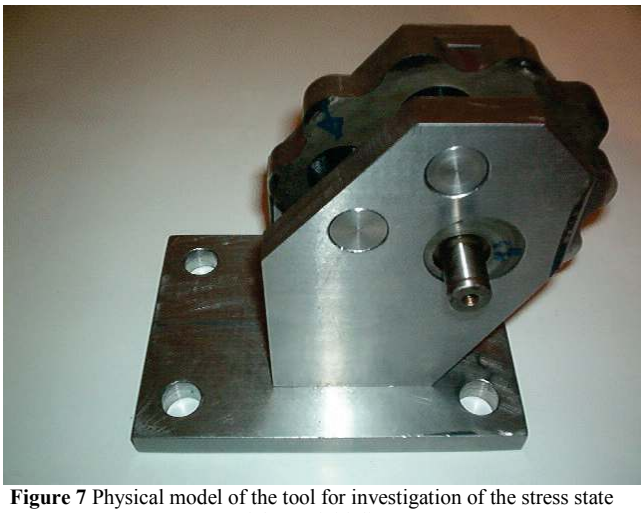

Figure 7 Physical model of the tool for investigation of the stress state of the cycloid disc

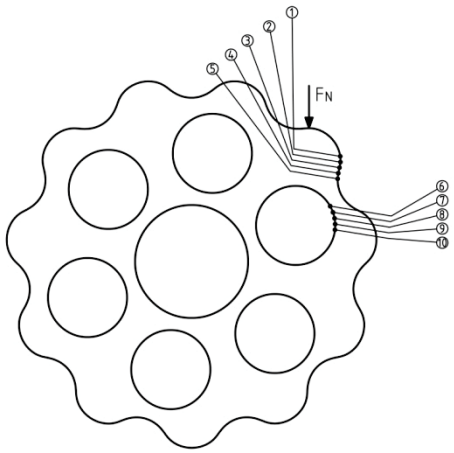

Figure 8 Schematic drawing of the cycloid disc with positions of the strain gauges

Strain gauges method was used in this investigation. Considering the dimensions of the cycloid disc and used strain gauges, values of strain were not possible to be measured in the contact zone itself, but in the nearest possible zone. Type 2/120 KY11 strain gauge chains produced by HBM were used. In total, 10 strain gauge chains were glued, divided into two groups, with 5 chains each, and with a constant distance of 2 mm, which provided adequate data acquisition [18]. Distribution of the strain gauge chains is given in Fig. 8 and the test table used for experimental analysis is shown in Fig. 9. Measuring was done in the Laboratory for Machine Elements at the Faculty of Engineering, University of Kragujevac.

As it was stated before, the normal force value on the cycloid disc teeth in case of single meshing is 4630 N. Measuring of the cycloid disc strain was done for the range of the normal force F_N values from 0 to 4830 N. Measuring was repeated three times in order to verify the results. Very similar results were obtained in all three measurements and therefore they can be considered as valid and reliable to evaluate stress state of the cycloid disc.

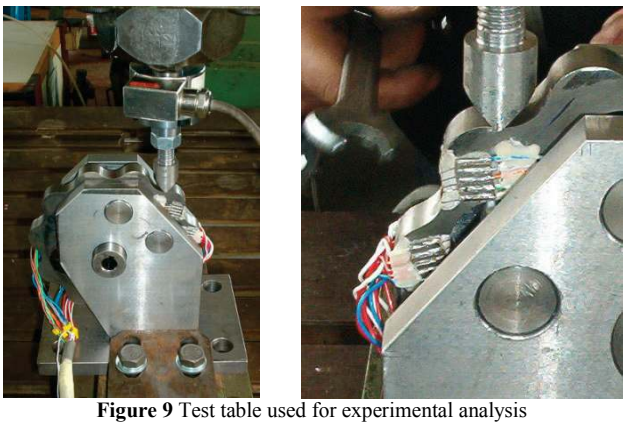

Figure 9 Test table used for experimental analysis

The values of the measured strain are given in Tab. 2, for all 10 set up locations foreseen for the normal force F_N in the range of 0 to 4830 N. It is easy to see that the highest values of the strain were obtained at positions of the strain gauge chain 5.

Based on the values of strain for the normal force F_N = 4630 N, normal stress values were calculated and given in Tab. 3. The stress values are also given in this table, for these same locations, determined by numerical calculations.

From Tab. 3, it is easy to observe that the maximum deviation between numerical values and experimentally determined stress values is 7,3 %, which is extremely good results matching.

Fig. 10 presents the diagram of strain values as a function of the strain gauge position, for the normal force value corresponding to the single meshing (F_N = 4630 N), while Fig. 11 shows comparative values of the numerically and experimentally obtained stresses.

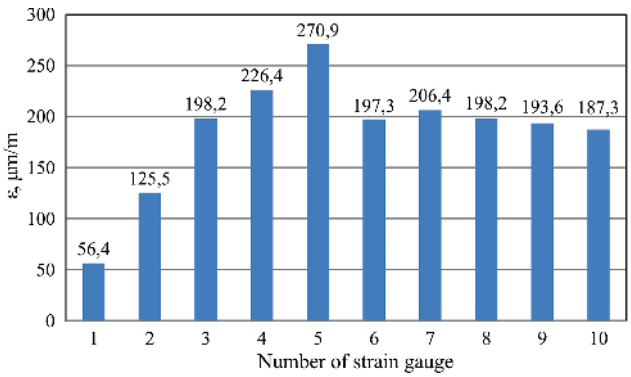

Figure 10 Diagram of the measured strain values

Table 2 Strain values obtained by measurements

F_N, N	ε_1 μm/m	ε_2 μm/m	ε_3 μm/m	ε_4 μm/m	ε_5 μm/m	ε_6 μm/m	ε_7 μm/m	ε_8 μm/m	ε_9 μm/m	ε_{10} μm/m
0	0,0	0,0	0,0	0,0	0,0	0,0	0,0	0,0	0,0	0,0
340	2,7	6,4	9,1	9,1	11,8	10,0	10,0	9,1	9,1	7,3
950	10,0	22,7	36,4	40,9	49,1	39,1	40,9	39,1	37,3	36,4
1130	11,8	27,3	43,6	49,1	59,1	46,4	49,1	46,4	45,5	43,6
1630	20,0	43,6	69,1	79,1	93,6	71,8	74,5	71,8	70,0	67,3
1890	23,6	51,8	80,9	93,6	110,9	83,6	86,4	82,7	80,9	77,3
1970	23,6	52,7	83,6	94,5	111,8	83,6	87,3	82,7	80,9	77,3
2020	24,5	55,5	87,3	100,0	119,1	90,0	93,6	90,0	88,2	85,5
2280	28,2	62,7	99,1	112,7	133,6	99,1	103,6	98,2	96,4	91,8
2310	28,2	62,7	99,1	112,7	133,6	99,1	103,6	98,2	96,4	91,8
2330	29,1	64,5	101,8	115,5	138,2	103,6	108,2	103,6	101,8	98,2
2580	31,8	71,8	112,7	129,1	154,5	114,5	120,0	114,5	112,7	109,1
2840	35,5	78,2	124,5	141,8	169,1	126,4	131,8	126,4	123,6	120,0
3100	38,2	85,5	135,5	154,5	183,6	135,5	141,8	135,5	132,7	128,2
3140	39,1	85,5	136,4	154,5	184,5	136,4	141,8	135,5	132,7	128,2
3160	39,1	87,3	139,1	159,1	189,1	140,0	146,4	140,9	138,2	133,6
3430	42,7	93,6	150,0	171,8	205,5	151,8	158,2	151,8	149,1	144,5
3520	43,6	96,4	152,7	174,5	208,2	152,7	159,1	152,7	149,1	144,5
3450	43,6	96,4	154,5	176,4	210,9	156,4	162,7	156,4	153,6	149,1
3780	47,3	104,5	166,4	190,0	226,4	166,4	172,7	166,4	162,7	156,4
3820	47,3	105,5	166,4	190,0	227,3	166,4	174,5	167,3	164,5	159,1
4010	50,0	110,9	176,4	200,0	240,0	175,5	182,7	175,5	171,8	165,5
4020	50,0	110,9	176,4	200,9	240,9	177,3	184,5	177,3	174,5	169,1
4150	51,8	114,5	181,8	207,3	247,3	181,8	189,1	180,9	177,3	171,8
4230	52,7	117,3	186,4	211,8	253,6	184,5	193,6	184,5	180,9	175,5
4290	53,6	119,1	189,1	215,5	258,2	188,2	196,4	188,2	183,6	178,2
4350	54,5	120,0	190,9	218,2	260,9	190,0	198,2	190,0	186,4	180,0
4370	54,5	120,9	192,7	219,1	262,7	190,9	200,0	191,8	187,3	180,9
4400	55,5	121,8	193,6	220,9	264,5	192,7	200,9	192,7	189,1	182,7
4440	55,5	122,7	195,5	222,7	267,3	194,5	202,7	194,5	190,9	183,6
4470	56,4	123,6	197,3	224,5	269,1	196,4	204,5	196,4	191,8	185,5
4490	56,4	124,5	198,2	225,5	270,0	196,4	205,5	197,3	192,7	186,4
4630	56,4	125,5	198,2	226,4	270,9	197,3	206,4	198,2	193,6	187,3
4720	58,2	127,3	200,0	229,1	273,6	198,2	209,1	200,0	194,5	189,1
4830	59,1	129,1	200,9	230,9	276,4	200,9	210,9	201,8	197,3	190,9

Table 3 Comparative values of the normal stress

Strain gauge chain	ε / μm/m (experimental value)	σ / MPa (experimental value)	σ / MPa (numerical value)	Deviation %
1	56,4	11,8	12,7	7,3
2	125,5	26,3	28,2	7,0
3	198,2	41,6	41,2	1,0
4	226,4	47,5	46,1	3,0
5	270,9	56,9	54,5	4,2
6	197,3	41,4	42,4	2,3
7	206,4	43,3	44,9	3,6
8	198,2	41,6	43,3	4,0
9	193,6	40,7	42,2	3,8
10	187,3	39,3	37,4	4,9

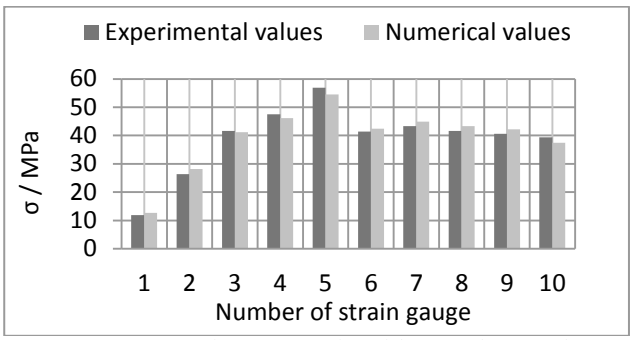

Figure 11 Comparative representation of the normal stress values obtained by experimental and numerical method

5 Conclusions

This paper presents the results of numerical and experimental analysis of the cycloid disc stress state for single meshing. Based on the obtained results, the following conclusions can be made:

a) Stress values obtained by using numerical and experimental methods were in exceptionally good agreement. That was verified that numerical models were well defined.
b) Maximum stress values occurred at the contact point of the cycloid disc tooth and the roller of the stationary central gear.
c) Maximum stress value is significantly below the allowed value, even for the most critical case of the meshing - single meshing. This is actually one of the most important advantages of the cycloidal profile meshing.

6 References

[1] Kudrijavcev, V. N. Planetary gear train, Mechanical Engineering, Leningrad, 1966, (in Russian).
[2] Lehmann, M. Calculation and measurement of forces acting on cycloid speed reducer, PhD Thesis, Technical University Munich, Germany, 1976, (in German).

[3] Malhotra, S. K.; Parameswaran, M. A. Analysis of a cycloid speed reducer. // Mechanism and Machine Theory. 18, 6(1983), pp. 491-499.
[4] Litvin, F.; Feng, P. Computerized design and generation of cycloidal gearings. // Mechanism and Machine Theory. 31, 7(1996), pp. 891-911.
[5] Yang, D. C. H.; Blanche, J. G. Design and application guidelines for cycloid drives with machining tolerances. // Mechanism and Machine Theory. 25, 5(1990), pp. 487-501.
[6] Tamizharasan, T.; Senthil Kumar, N. Optimization of Cutting Insert Geometry Using DEFORM-3D: Numerical Simulation and Experimental Validation. // International Journal of Simulation Modelling. 11, 2(2012), pp. 65-76
[7] Metalsi Tani, F.; Bourdim, A. Study of feasibility of plastic gear to reduce noise in a gear pump. // Advances in Production Engineering & Management. 7, 2(2012), pp. 143-149
[8] Deng, W. J.; Xie, Z. C.; Li, Q.; Lin, P. Finite Element Modelling and Simulation of Chip Breaking with Grooved Tool. // International Journal of Simulation Modelling. 12, 4(2013), pp. 264-275
[9] Chmurawa, M.; Lokiec, A. Distribution of loads in cycloidal planetary gear (CYCLO) including modification of equidistant, 16th European ADAMS user conference, Berchtesgaden, Germany, 2001.
[10] Chmurawa, M.; John, A. Numerical analysis of forces, stress and strain in planetary wheel of cycloidal gear using FEM. // Journal of Mechanical Engineering. 53, 2(2002), pp. 77-92.
[11] Blagojevic, M. Stress and strain state of cyclo speed reducer's elements under dynamic loads, PhD Thesis, Faculty of Engineering Kragujevac, Serbia, 2008, (in Serbian).
[12] Blagojevic, M.; Marjanovic, N.; Djordjevic, Z.; Stojanovic, B. Stress and strain state of single-stage cycloidal speed reducer. // The 7th International Conference Research and Development of Mechanical Elements and Systems, Zlatibor, Serbia, 2011, pp. 553-558.
[13] Blagojevic, M.; Marjanovic, N.; Djordjevic, Z.; Stojanovic, B.; Disic, A. A new design of a two-stage cycloidal speed reducer. // Journal of Mechanical Design. 133, 8(2011).
[14] Meng, Y.; Wu, C.; Ling, L. Mathematical modeling of the transmission performance of 2K-H pin cycloid planetary mechanism. // Mechanism and Machine Theory. 42, 7(2007), pp. 776-790.
[15] Gorla, C.; Davoli, P.; Rosa, F.; Longoni, C.; Chiozzi, F.; Samarani, A. Theoretical and experimental analysis of a cycloidal speed reducer. // Journal of Mechanical Design, 130, (2010).
[16] Sensiger, J. W. Unified approach to cycloid drive profile, stress and efficiency optimization. // Journal of Mechanical Design. 132, 2(2010).
[17] Ivanovic, L.; Devedzic, G.; Miric, N.; Cukovic, S. Analysis of forces and moments in gerotor pumps. // Journal of Mechanical Engineering Science (Part C). 224, (2010), pp. 2257-2269.
[18] Hoffmann, K. An introduction to measurements using strain gages, Darmstadt, Germany, 1989.

Authors' addresses

Associate Prof. Mirko Blagojevic, Ph.D.
Faculty of Engineering,
University of Kragujevac,
S. Janjić 6, RS-34000 Kragujevac, Serbia
E-mail: mirkob@kg.ac.rs

Full Prof. Nenad Marjanovic, Ph.D.
Faculty of Engineering,
University of Kragujevac,
S. Janjić 6, RS-34000 Kragujevac, Serbia
E-mail: nesam@kg.ac.rs

Zorica Djordjevic, Ph.D., Associate Prof.
Faculty of Engineering,
University of Kragujevac,
S. Janjić 6, RS-34000 Kragujevac, Serbia
E-mail: zoricadj@kg.ac.rs

Blaza Stojanovic, Ph.D., Assistant Prof.
Faculty of Engineering,
University of Kragujevac,
S. Janjić 6, RS-34000 Kragujevac, Serbia
E-mail: blaza@kg.ac.rs

Vesna Marjanovic, Ph.D., Assistant Prof.
Faculty of Engineering,
University of Kragujevac,
S. Janjić 6, RS-34000 Kragujevac, Serbia
E-mail: vmarjanovic@kg.ac.rs

Rodoljub Vujanac, M.Sc., Assistant
Faculty of Engineering,
University of Kragujevac,
S. Janjić 6, RS-34000 Kragujevac, Serbia
E-mail: vujanac@kg.ac.rs

Aleksandar Disic, Ph.D. student, Assist.
Faculty of Engineering,
University of Kragujevac,
S. Janjić 6, RS-34000 Kragujevac, Serbia
E-mail: disic@kg.ac.rs